singlet–triplet transition moments which are required to fit the relative intensities of the lines in the laser-induced phosphorescence spectrum. However, the major consequences of the discovery that excited triplet states of polyatomic molecules can be prepared with rotational state selection under collision-free conditions is likely to be dynamic, rather than structural, in nature. Glyoxal is only one of several different molecules in which triplet states appear to participate in, and in some cases dominate, the internal "radiationless" energy flow.[9] All previous experimental studies of these processes have involved the initial preparation of singlet states followed by "intersystem crossing" into isoenergetic states high in the triplet manifold,[10] and therefore suffer from various types of perturbations that may obscure and/or modify the true intramolecular behavior. To be sure, such studies are valuable; they have revealed, for example, an important discrepancy between the gas-phase triplet decay rate extrapolated to zero excess energy and that measured in crystals at low temperatures.[11] But detailed information about the origins of these effects can only be obtained if state-selected, "pure" triplets are first prepared and then studied as a function of vibrational and rotational energy content. Direct access to the triplet manifold will also facilitate studies of other dynamic processes, including T_1/S_0 and T_1/T_n interstate couplings, vibrational and rotational relaxation, and photodissociation, all on a much longer time scale than is possible with "pure" singlet states. Experiments of this type will be difficult, but not impossible, using the approach described in this Letter.

Acknowledgment. Many persons have contributed to the success of this experiment, both directly and indirectly. Ms. Wendy Butler synthesized glyoxal and Ms. Leanne Henry wrote the program which aided us in the interpretation of the spectrum. We thank them both. We are also grateful to Professors K. K. Innes, J. Kommandeur, M. E. Michel-Beyerle, R. E. Smalley, A. Tramer, and J. H. van der Waals for encouragement. This work was supported by the Research Corporation, the North Atlantic Treaty Organization (31.80/DI), and the National Science Foundation (CHE-8021082).

(9) For a review, see Ph. Avouris, W. M. Gelbart, and M. A. El-Sayed, *Chem. Rev.*, 77, 793 (1977).
(10) See, for example, Y. Matsumoto, L. H. Spangler, and D. W. Pratt, *Chem. Phys. Lett.*, 98, 333 (1983), and references contained therein.
(11) R. E. Smalley, *J. Phys. Chem.*, 86, 3504 (1982).

FEATURE ARTICLE

Symmetry Breaking in Polyatomic Molecules: Real and Artifactual

Ernest R. Davidson* and Weston Thatcher Borden

Chemistry Department BG-10, University of Washington, Seattle, Washington 98195 *(Received: May 31, 1983)*

A review is presented of recent work by the authors and their collaborators on molecules with broken symmetry. Examples are given in which the symmetry breaking arises from Von Neumann–Wigner or Jahn–Teller avoided intersections or from pseudo-Jahn–Teller effects. Examples are also cited in which approximate wave functions show broken symmetry at symmetrical arrangements of the nuclei. Such calculations necessarily, and often incorrectly, predict distorted equilibrium geometries.

Potential surfaces are of importance in chemistry for explaining geometries, spectra, and chemical reactions. Potential surfaces for molecules which could be of high symmetry may display minima of lower symmetry that are induced by degeneracies or near degeneracies. The effects of avoided crossings in diatomic molecules are fairly well characterized, but intersections of polyatomic potential surfaces are still only vaguely understood. While the general type of features to be expected are well-known, the actual appearance of these structures in potential surfaces is still often regarded with surprise and is frequently overlooked.

Although the potential surfaces for the ground states of closed-shell molecules seldom display much structure near the equilibrium geometry, the potential surfaces for excited states and for open-shell molecules often display large amounts of structure because of the closer spacing of the electronic states. Examples of some of these highly structured surfaces, gleaned from recent work done in this laboratory, will be presented in this review.

The structure of the polyatomic potential surface and related wave function in the neighborhood of an intersection has been described in the papers of Von Neumann and Wigner, Jahn and Teller, and Herzberg and Longuet-Higgins. The surface in every case exhibits a double cone structure when plotted against an appropriate pair of coordinates. The locus of nuclear coordinates over which degeneracy persists is of dimensionality $3N - 8$ in the $3N - 6$ dimensional space of internal coordinates. Davidson has discussed the locus of degeneracy on the ground-state surface for several triatomic radicals.

The paper of Von Neumann and Wigner[1] described the case of degeneracy due to "accidental" crossing of surfaces, while Jahn and Teller[2] described the structure near a point

(1) Neumann, J. V.; Wigner, E. P. *Z. Phys.* **1929**, *30*, 467.

0022-3654/83/2087-4783$01.50/0

of "intrinsic" (i.e., group theory imposed) degeneracy. The potential surface has a double cone structure for small displacements from the high symmetry point and a low energy trough encircling the peak. Many examples of the Jahn–Teller theorem have been discussed, and tomes[3] have been written on the resulting pseudo-rotation vibrational structure. The more general case discussed by Von Neumann and Wigner, and illustrated for the HNO molecule by Herzberg and Longuet-Higgins,[4] is usually overlooked. Many examples are now known where potential surfaces for states of different spatial symmetry intersect when plotted against a symmetry-preserving coordinate. If some symmetry-breaking coordinate causes the states to belong to the same representation in a lower symmetry point group, then the intersecting surfaces will usually appear as a double cone when plotted against these two coordinates.

General Considerations

Broken symmetry structures may appear as minima on a calculated potential surface for several reasons. One of the most common is that the calculation is "wrong". That is, the form assumed for the wave function is oversimplified and leads to artifactual structure on the potential surface. It is easily demonstrated that any exact eigenfunction of an electronic Hamiltonian in the Born–Oppenheimer approximation must belong to an irreducible representation of the point group of the Hamiltonian. If an approximate functional form (such as a single Slater determinant) is assumed for the wave function, optimization of the average energy of this function may lead to a function that does not have pure symmetry (i.e., which does not transform like any irreducible representation under the operations of the group). Spin symmetry (as in unrestricted Hartree–Fock (UHF) calculations), time reversal symmetry (leading to complex wave functions even when the Hamiltonian is real), as well as point group symmetry may all be broken. Symmetry can always be imposed as a boundary condition during the optimization of the wave function. This is commonly done for spin and time reversal symmetry. Imposition of spatial symmetry, however, often leads to discontinuities on the potential surface since only certain geometrical arrangements have any symmetry.[5] In order to obtain a continuous potential surface, the same prescription for obtaining the energy must be used at every point.

Even if symmetry constraints are not imposed on the wave function, the potential surface may still not be smooth. If at a point of high symmetry the optimized wave function does not belong to any irreducible representation of the point group, then application of the point group operators will generate related wave functions. Even for a nondegenerate state these related functions will all have the same energy. The energy will then show an artifactual cusp at the symmetrical point and the minimum energy will occur for a distorted geometry. Further, the wave function will change discontinuously as the molecule is distorted in different directions. While many molecules really are unsymmetrical, prediction of this loss of symmetry with a wave function which is incorrect at the symmetrical geometry destroys the credibility of the prediction.

For a state which should be degenerate, the behavior may be more bizarre. If the optimized partner wave functions in a degenerate representation break symmetry in such a way that they do not in fact transform as partners under the point group, then their energies will not be degenerate, and the correct Jahn–Teller cone shape of the potential surface will not be found. In such a case the pseudo-rotation trough may have minima and maxima at positions reversed from those on the correct surface, so that the predicted equilibrium geometry is entirely wrong. Unfortunately, for symmetry-unconstrained calculations, very high-quality wave functions are usually required before partner functions display the correct degeneracy.

Even calculations of sufficient quality to produce smooth potential surfaces with wave functions of the correct symmetry may still be qualitatively incorrect. When there is more than one equivalent valence bond structure that can be drawn, there is always a competition between distortion of the molecule to the bond lengths appropriate for one of the structures and resonance among the various structures at a geometry inappropriate to each of them. Often molecular orbital wave functions, even with configuration interaction (CI), are unable to describe all the equivalent valence bond structures simultaneously with equal accuracy. Consequently, such wave functions can lead to incorrect predictions of geometry. Molecular orbital calculations with only a low level of CI may also overestimate the amount of electron repulsion in a delocalized wave function and lead to an incorrect prediction of bond alternation in unsaturated molecules.

Although incorrect behavior of the wave function is easiest to detect in molecules which have a possible geometry of high symmetry, the phenomenon is not actually symmetry related. Completely unsymmetrical molecules can also have geometries at which there is more than one optimal wave function of a limited functional form with the same energy. In such a case the potential surface will incorrectly display a cusp, and the calculated wave function will be discontinuous.

The Von Neumann–Wigner Theorem

Von Neumann and Wigner originally proved the fundamental theorem related to the question of degeneracy in molecules. If one assumes the nonrelativistic Born–Oppenheimer separation, as it is now conventionally understood, the electronic Hamiltonian is then real; and its eigenvalues as a function of the nuclear coordinates are the potential surfaces of the molecule. For two arbitrary functions of K parameters the surface of intersection would almost always be of dimensionality $K - 1$. Von Neumann and Wigner showed that two potential surfaces obtained from a Hamiltonian which depends on K parameters will almost always intersect in a surface of dimensionality $K - 2$. Further, they showed that when the parameters are selected correctly, the potential surfaces will display a double cone structure when plotted against the other two parameters.

The phrase "almost always" in the above statement refers to all conceivable Hamiltonians except for a subset of measure zero. Isolated exceptions can of course be artificially constructed but are unlikely to occur in actual molecules. Teller[6] applied this theorem to derive the "noncrossing" rule for diatomic molecules, and Jahn and Teller[2] used the theorem to demonstrate by enumeration that degeneracy induced by point group symmetry can always be removed by a symmetry lowering distortion that leads to a lower energy. Herzberg and Longuet-Higgins[4,7] carried the theorem one step further and showed that the

(2) Jahn, H. A.; Teller, E. *Proc. R. Soc. London, Ser. A* **1937**, *161*, 220.
(3) See, for example, Englman, R. "The Jahn Teller Effect in Molecules and Crystals"; Wiley-Interscience: New York, 1972.
(4) Herzberg, G. H.; Longuet-Higgins, A. C. *Discuss. Faraday Soc.* **1963**, *35*, 77.
(5) Manne, R. *Mol. Phys.* **1972**, *24*, 935.
(6) Teller, E. *J. Phys. Chem.* **1937**, *41*, 209.
(7) Longuet-Higgins, H. C. *Proc. R. Soc. London, Sec. A* **1975**, *344*, 147.

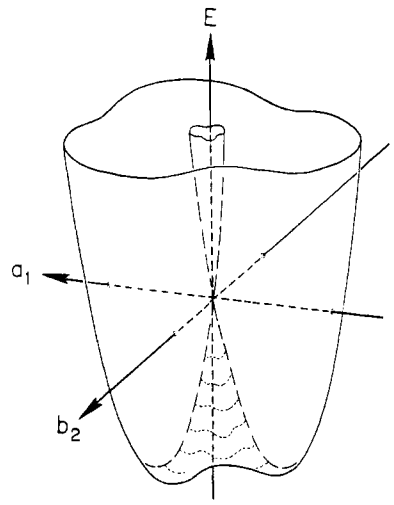

Figure 1. A typical Jahn–Teller potential surface for an E state distorted by an e vibration in a molecule with a C_3 axis perpendicular to the vibrational motion. The energy, E, is plotted against the two components, a_1 and b_2, of the vibration.

electronic wave function could not be made a continuous function of nuclear coordinates on a circle around the point of intersection. Liehr[8] also considered motion on this circle for the case of symmetry breaking and worked out many examples of the type of pseudo-rotation motion expected for a Jahn–Teller distorted molecule.

To understand the so-called second-order Jahn–Teller effect it is useful to consider a heuristic discussion of the Jahn–Teller theorem. If two states are degenerate at some point, and Q_1 and Q_2 are distortions chosen so that the Hamiltonian matrix elements H_{11} and H_{22} are linear in Q_1 with equal and opposite slopes, and H_{12} is linear in Q_2 with the same slope, then

$$\begin{bmatrix} E^0 + \alpha Q_1 & \alpha Q_2 \\ \alpha Q_2 & E^0 - \alpha Q_1 \end{bmatrix} \begin{bmatrix} c_1 \\ c_2 \end{bmatrix} = E \begin{bmatrix} c_1 \\ c_2 \end{bmatrix} \tag{1}$$

The solution to this gives

$$E = E^0 \pm |\alpha|[Q_1^2 + Q_2^2]^{1/2} \tag{2}$$

This is the ordinary Jahn–Teller situation which gives rise to the double cone potential surface depicted in Figure 1. Now suppose the states are nondegenerate and of different symmetry. Then the diagonal elements must be quadratic in any symmetry-breaking distortion, Q_2. If we consider only Q_2, the off-diagonal element may still be linear so that

$$\begin{bmatrix} E_1^0 + k_1 Q_2^2 & \alpha Q_2 \\ \alpha Q_2 & E_2^0 + k_2 Q_2^2 \end{bmatrix} \begin{bmatrix} c_1 \\ c_2 \end{bmatrix} = E \begin{bmatrix} c_1 \\ c_2 \end{bmatrix} \tag{3}$$

which gives, to second order in Q_2

$$E_1 = E_1^0 + Q_2^2[k_1 - \alpha^2/(E_2^0 - E_1^0)] \tag{4}$$

In this second-order Jahn–Teller case the interesting question is the sign of the resultant force constant for distortion along Q_2. If this is positive, the molecule will be symmetrical, while if it is negative the molecule will be unsymmetrical. The preferred geometry will depend on the difference $E_2^0 - E_1^0$ and on α, both of which may vary with other coordinates.

Examples

Jahn–Teller Distortions. The simplest example of a Jahn–Teller distortion involves a ^2E state of a molecule with D_{3h} symmetry and an e_1 vibrational mode. We have discussed this situation for H_3,[9] Na_3,[10] and C_3H_3[11] (cyclopropenyl radical). In all of these cases the electronic wave function has only one electron in a degenerate e orbital. If the C_{2v} subgroup of D_{3h} with the C_2 axis along the y direction is arbitrarily selected, the partner wave functions (Φ_x, Φ_y) for the E representation can be chosen to transform like (B_2, A_1) and (A_2, B_1) for the standard e_x and e_y σ and π orbitals, respectively. Similarly the in-plane E vibrations will transform like (b_2, a_1). The diagonal elements of a 2×2 Hamiltonian are then linear in the Q_y distortion, while the off-diagonal element is linear in Q_x. Further, by the generalized Wigner–Eckart theorem, the proportionality factor is the same, so H has the form

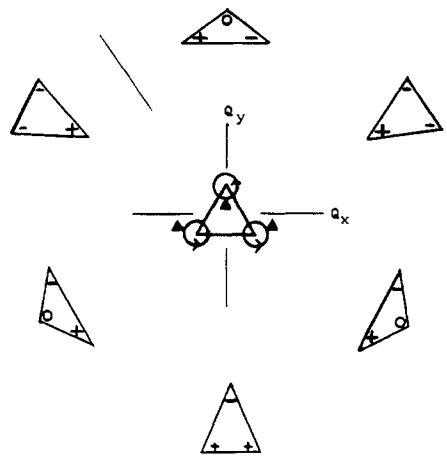

Figure 2. The variation in the sign pattern of the singly occupied orbital of Na_3, H_3, and C_3H_3 as a function of in-plane distortions of symmetry e′.

$$\begin{bmatrix} E^0 + \alpha Q_y & \alpha Q_x \\ \alpha Q_x & E^0 - \alpha Q_y \end{bmatrix}$$

and the energies and wave functions take the form

$$E = E^0 \pm \alpha Q \tag{5}$$

$$\Psi_1 = \cos(\chi/2)\Phi_x + \sin(\chi/2)\Phi_y$$

$$\Psi_2 = -\sin(\chi/2)\Phi_x + \cos(\chi/2)\Phi_y \tag{6}$$

in terms of the pseudo-rotation coordinates

$$Q^2 = Q_x^2 + Q_y^2$$

$$\tan\chi = Q_x/Q_y \tag{7}$$

For noninfinitesimal displacements these equations must be modified by higher order effects. These effects will lead to a minimum energy trough for some value of Q and to minima and maxima along the pseudo-rotation path in this trough as χ is varied.

For H_3 the potential surface[9] for a fixed distortion amplitude Q has six equivalent linear minima of the form H_2···H. The potential surface is repulsive, however, and has its absolute minimum at infinite Q. For Na_3 and other group 1A and 1B trimers the situation is quite different.[10] The minima occur at three equivalent obtuse triangle shapes with $^2B_2$ wave functions. Maxima for pseudo-rotation occur at three acute triangle shapes with $^2A_1$ wave functions. Although the potential surface for pseudo-ro-

(8) Liehr, A. D. *J. Phys. Chem.* **1963**, *67*, 389.

(9) Davidson, E. R. *J. Am. Chem. Soc.* **1977**, *99*, 397.
(10) Martin, R. L.; Davidson, E. R. *Mol. Phys.* **1978**, *35*, 1713.
(11) Davidson, E. R.; Borden, W. T. *J. Chem. Phys.* **1977**, *67*, 2191.

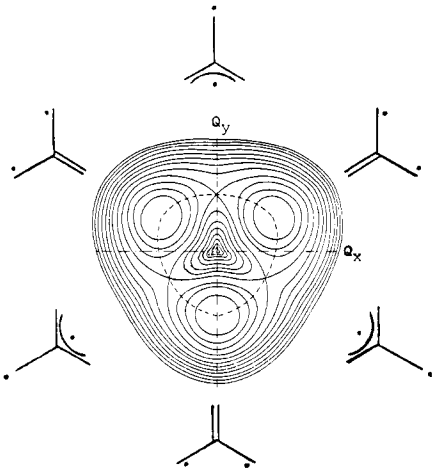

Figure 3. A schematic representation of the wave functions and potential energy surface for $^1E'$ trimethylenemethane as a function of e′ stretching of the CC bonds.

tation is quite flat, the rather large mass of Na results in the existence of a few pseudo-rotation levels below the barrier. For experiments which are fast compared to the tunneling rate, the molecule at low temperature will seem to be obtuse. Figure 2 illustrates how the orbital containing the unpaired electron varies around the pseudo-rotation valley for the ^2E state. This figure also shows the sign discontinuity in this orbital. Also included is a sketch of the type emphasized by Liehr, showing the actual motion of the nuclei.

For the cyclopropenyl radical[11] the roles of the obtuse and acute triangles are reversed, although the sign pattern for the π orbital containing the unpaired electron is the same as shown in Figure 2. In the planar molecule three equivalent acute triangles with $^2B_1$ wave functions represent the minima along the pseudo-rotation path and three equivalent obtuse triangles with $^2A_2$ wave functions correspond to the transition states connecting the minima. The potential surface for the planar molecule is rather flat; but pyramidalization of the unique carbon in the $^2B_1$ state, in which the unpaired electron is localized at this carbon, results in further stabilization of the minima on the pseudo-rotation surface.[12] Recent experiments by Closs are in good agreement with not only the location but also the predicted depth of the minima on the surface.[13]

Degenerate states also arise at D_{3h} geometries for molecules in which two electrons occupy a degenerate pair of orbitals.[14] Such molecules that have been studied by us include $C(CH_2)_3$ (trimethylenemethane),[15] $C_3H_3^-$ (cyclopropenyl anion),[11] and the isoelectronic[16] $(NH)_3^{2+}$. The double occupancy of an e″ set of π orbitals gives rise to $^3A_2'$, $^1E'$, and $^1A_1'$ states. The presence of the latter singlet state may give rise to a strong second-order Jahn–Teller effect. These second-order effects produce maxima and minima along the pseudo-rotation pathway for the lowest singlet state, and the location of these extrema can readily be predicted.

For example, in planar trimethylenemethane (TMM), the two components of $^1E'$ can be represented schematically as shown in Figure 3. The $^1E_x'$ component resembles an allylic radical with the second unpaired electron localized at the remaining peripheral carbon, whereas $^1E_y'$ has a strong π bond to this carbon and rather weak π bonds to the remaining two carbons, where the nonbonding electrons are largely localized.

This representation of the $^1E'$ state makes the energy matrix diagonal in a Q_y distortion, one phase of which lengthens the bond to the unique peripheral carbon atom and shortens the bonds to the other two carbons. This distortion from D_{3h} symmetry causes a first-order stabilization of $^1E_x'$, while destabilizing $^1E_y'$. Because of the linearity in Q_y, the negative of this distortion destabilizes the former component of $^1E'$ while stabilizing the latter. A Q_x distortion, which shortens one of the two equivalent bonds while lengthening the other, mixes the two components of $^1E'$ while producing the same amount of energy splitting as a Q_y distortion. This first-order effect is substantial, lowering the energy by about 8 kcal/mol after distortion from the optimal D_{3h} geometry to the C_{2v} geometry that is optimal for $^1B_2(^1E_x')$. Nevertheless, the effect vanishes for the symmetry-constrained spin-restricted Hartree–Fock (RHF) and two-configuration self-consistent-field (TCSCF) wave functions, and it is overshadowed by artifactual effects in the unconstrained RHF and TCSCF wave functions. This illustrates how important proper wave functions are to the correct description of first-order Jahn–Teller effects. In the case of trimethylenemethane full CI in the π space suffices.

The second-order effect arises because an E′ distortion mixes $^1A_1'$ with $^1E'$. More specifically, the mixing stabilizes $^1E_y'$ on a $\pm Q_y$ distortion and $^1E_x'$ on $\pm Q_x$. Since $^1E_y'$ is stabilized by both first- and second-order Jahn–Teller effects on $-Q_y$ distortions, while $^1E_x'$ is stabilized only by the first-order effect on $+Q_y$, it is possible to predict unequivocally that the minima on the potential surface for the planar TMM diradical should occur at the three equivalent $-Q_y$ distorted geometries for $^1E_y'$ type wave functions. This is shown in the schematic contour map of the potential surface in Figure 3. The three transition states connecting the minima on the lowest energy pseudo-rotation pathway correspond to $+Q_y$ distorted geometries with $^1E_{x'}$ type wave functions. The equivalent $\pm Q_x$ distortions lead to points on the pathway with intermediate energies; for although the second-order effect stabilizes $^1E_{x'}$ on such a distortion, the first-order effect causes the wave function to be a mixture of $^1E_{x'}$ and $^1E_{y'}$.

The location of the three equivalent minima on the potential surface for the planar cyclopropenyl anion, which is also an $(e'')^2$ molecule, can be predicted unequivocally by similar types of considerations involving first- and second-order Jahn–Teller effects.[11] However, two-configuration SCF calculations on either the anion or on the isoelectronic $(NH)_3^{2+}$ in C_{2v} symmetry showed a minimum for the opposite phase of the Q_y distortion from that expected.[16] These molecules have very nonuniform π electron distributions which lead to large σ polarization. At the SCF or π MCSCF level of description this leads to loss of degeneracy at D_{3h} geometries. A symmetry analysis demonstrated that CI wave functions that provided for correlation of the σ electrons with the π electrons were necessary to obtain pure $^1E'$ components in these ions. When the calculations were repeated with such wave functions, the minima on the potential surfaces for the

(12) Poppinger, D.; Radom, L.; Vincent, M. A. *Chem. Phys.* **1977**, *23*, 437.
(13) Closs, G. L.; Evanochko, T.; Norris, J. R. *J. Am. Chem. Soc.* **1982**, *104*, 350.
(14) Borden, W. T.; Davidson, E. R. *Acc. Chem. Res.* **1981**, *14*, 69. Borden, W. T.; Davidson, E. R.; Feller, D. *Tetrahedron*, **1982**, *38*, 737. Borden, W. T.; In "Diradicals"; Borden, W. T., Ed.; Wiley-Interscience: New York, 1982; Chapter 1, pp 1–72.
(15) Borden, W. T. *J. Am. Chem. Soc.* **1976**, *98*, 2695. Davidson, E. R.; Borden, W. T. *J. Chem. Phys.* **1976**, *64*, 663. *J. Am. Chem. Soc.* **1977**, *99*, 2053. Feller, D.; Tanaka, K.; Davidson, E. R.; Borden, W. T. *Ibid.* **1982**, *104*, 967. Feller, D.; Borden, W. T.; Davidson, E. R. *J. Chem. Phys.* **1981**, *74*, 2256.
(16) Borden, W. T.; Davidson, E. R.; Feller, D. *J. Am. Chem. Soc.* **1980**, *102*, 5302.

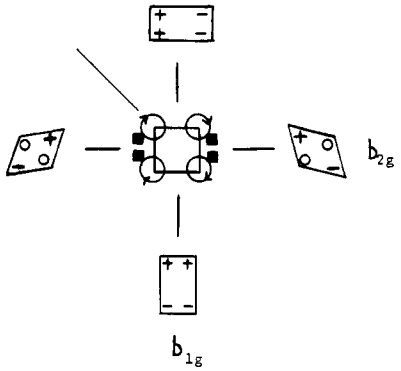

Figure 4. The variation in the singly occupied orbital of cyclobutadiene radical cation as a function of b_{1g} and b_{2g} carbon framework distortions.

planar ions appeared at the expected locations, corresponding to obtuse triangles with π wave functions resembling those for allylic anions.

Both TMM and cyclopropenylanion [and the isoelectronic $(NH)_3^{2+}$] illustrate that global minima on potential surfaces do not necessarily have the same type of wave functions as the local minima found on some subsurface. In TMM the lowest singlet diradical has an $^1E_x'$ type wave function with the unique methylene group twisted out of conjugation, instead of the $^1E_y'$ wave function preferred by the planar molecule. In cyclopropenyl anion [and $(NH)_3^{2+}$] pyramidalization of the unique atom of the three-membered ring stabilizes a wave function that localizes a pair of electrons at this atom at an acute triangular geometry. Pyramidalization transforms such a wave function from lying on the upper Jahn–Teller surface for the planar molecule to being one of the equivalent minima on the global surface.[16]

Degenerate orbitals also occur in molecules with symmetry axes higher than threefold. We have carried out calculations on potential surfaces for molecules that belong to D_{4h} and D_{5h} point groups. The molecules examined were planar cyclobutadiene and its radical cation and planar cyclopentadienyl cation and radical.

Cyclobutadiene radical cation[17] has one electron in a degenerate e_g orbital. Group theory predicts that the degeneracy of the resulting ^2E_g state can be lifted by a b_{1g} or b_{2g} distortion from D_{4h} symmetry. The former distortion transforms the square molecule into one of two equivalent rectangles, while the latter takes it into one of two equivalent rhombuses. Since the two types of distortions are nonequivalent, one leads to the pair of minima on the potential surface, and the other leads to the pair of transition states on the pseudo-rotation pathway that connects the minima. From the behavior of the singly occupied orbital, shown in Figure 4, one would expect the rectangular form to be stabilized due to the enhanced nearest-neighbor bonding vs. antibonding interactions. The trapezoid form would be anticipated to change less in energy because it has no nearest-neighbor orbital interactions.

In order to establish computationally which distortion leads to which type of stationary point, it is necessary to carry out calculations in two different D_{2h} subgroups of D_{4h}. To assure that the results are not artifactually prejudiced, it is essential to demonstrate that the same D_{4h} energy is obtained for the radical cation regardless of which subgroup, if any, is used for the calculation. Because of the effect of the asymmetric distribution of π electrons on the σ core, it again proved necessary to carry out calculations that included both σ and π correlation in order to obtain the required invariance of the D_{4h} energy to the subgroup chosen. It was found that the b_{1g} (rectangular) distortion did, in fact, lead to the mimina on the potential surface for the radical cation. Interestingly, if either the RHF or UHF energies (rather than the σ–π CI energies) of the rectangularly and rhomboidally distorted geometries were compared, one would have erroneously arrived at the opposite conclusion.

Figure 5. Two ways to choose the degenerate e_1'' π orbitals for cyclobutadiene.

In the neutral cyclobutadiene molecule two electrons occupy the e_g MOs. This gives rise to four, low-lying, nondegenerate states—$^3A_{2g}$, $^1B_{1g}$, $^1A_{1g}$, and $^1B_{2g}$. In terms of the orbitals depicted in Figure 5 the wave functions may be written in two alternative forms:

$$^3A_{2g} = {}^3(e_xe_y) = {}^3(f_xf_y)$$

$$^1B_{1g} = {}^1(e_x^2 - e_y^2) = {}^1(f_xf_y)$$

$$^1B_{2g} = {}^1(e_xe_y) = {}^1(f_x^2 - f_y^2)$$

$$^1A_{1g} = {}^1(e_x^2 + e_y^2) = {}^1(f_x^2 + f_y^2)$$

Since there is no degeneracy, there are no first-order Jahn–Teller effects in these states of cyclobutadiene; only second-order effects are possible. The most important of these involves mixing of the $^1B_{1g}$ ground state with $^1A_{1g}$ under the influence of a b_{1g} distortion from a square to a rectangular geometry. Several different ab initio calculations have found this distortion to be energetically favorable, leading to the prediction that cyclobutadiene should adopt one of two equivalent rectangular geometries, which can interconvert via a square transition state.[18-21] Spectroscopic[22] and chemical trapping studies[23] have provided evidence for the correctness of these computational results.

Also of importance for cyclobutadiene is the fact that the $^1B_{2g}$ lies below $^3A_{2g}$, even at the D_{4h} geometry, in violation of Hund's rules. This effect is due to the Brillouin allowed single excitations in the open-shell $^1B_{1g}$ state[24] and has been named "dynamic spin polarization".[25]

Because the distortion of square cyclobutadiene to a rectangular geometry is a second-order Jahn–Teller effect, it was possible a priori that the molecule might have preferred a square geometry and had a positive force constant for rectangular distortion. In fact, the initial X-ray structure of tetra-*tert*-butylcyclobutadiene showed a geometry with all bond lengths in the four-membered ring nearly equal.[26a] However, a recent redetermination

(17) Borden, W. T.; Davidson, E. R.; Feller, D. *J. Am. Chem. Soc.* **1981**, *103*, 5725.

(18) Borden, W. T.; Davidson, E. R.; Hart, P. *J. Am. Chem. Soc.* **1978**, *100*, 388.
(19) Kollmar, H.; Staemmler, V. *J. Am. Chem. Soc.* **1977**, *99*, 3583.
(20) Buenker, R. J.; Peyerimhoff, S. D. *J. Chem. Phys.* **1968**, *48*, 354.
(21) Jafri, J. A.; Newton, M. D. *J. Am. Chem. Soc.* **1978**, *100*, 5012.
(22) Masamune, S.; Nakamura, N.; Suda, M.; Ona, H. *J. Am. Chem. Soc.* **1973**, *95*, 8481.
(23) Whitman, D. W.; Carpenter, B. K. *J. Am. Chem. Soc.* **1980**, *102*, 4272.
(24) Borden, W. T. *J. Am. Chem. Soc.* **1975**, *97*, 5968.
(25) Kollmar, H.; Staemmler, V. *Theor. Chim. Acta* **1978**, *48*, 223.
(26) (a) Irngartinger, H.; Riegler, N.; Malsch, K. D.; Schneider, K. A.; Maier, G. *Agnew. Chem., Int. Ed. Engl.* **1980**, *19*, 211. (b) Irngartinger, H.; Nixdorf, M. *Ibid.* **1983**, *22*, 403.

at lower temperatures showed more substantial bond length bond length alternation.[26b] It can be shown that single bond shortening should accompany double bond lengthening,[27] as is observed experimentally.

In contrast, distortion to a rectangular geometry in the cyclobutadiene radical cation is a first-order Jahn–Teller effect. Consequently, the cation cannot have a square geometry. Thus it can be predicted unequivocally that, unlike the neutral molecule, the tetra-*tert*-butylcyclobutadiene radical cation is not square.

A first-order Jahn–Teller effect is also predicted for cyclopentadienyl radical,[28] in which three π electrons occupy a degenerate pair of e_1'' orbitals, thus giving rise to a $^2E_1''$ state. A distortion of e_2' symmetry lifts the degeneracy of the two components of this state that occurs at D_{5h} geometries. It was found computationally that both phases of the e_y component of this distortion, which preserves C_{2v} symmetry, produce essentially the same energy lowering, although a different component of $^2E_1''$ is stabilized by the positive and negative phases. Thus, it appears that pseudo-rotation in the radical should be nearly unimpeded by barriers along the lowest energy pathway. Experimentally, the spin distribution around the ring is uniform on the EPR time scale at temperatures down to 120 K,[29] although pseudo-rotation is apparently frozen out at 70 K.

The cyclopentadienyl cation has one fewer π electrons than the radical, giving rise to $^3A_2'$, $^1A_1'$, and $^1E_2'$ states. The $^1E_2'$ state is expected to be the lowest singlet. It should show first-order Jahn–Teller activity on an e_1' distortion from D_{5h} symmetry and a second-order Jahn–Teller effect on an e_2' distortion, which allows mixing with the $^1A_1'$ state. Potential surface calculations show that the first-order Jahn–Teller effect is negligible in the cation but that the second-order effect plays a major role in stabilizing the lowest singlet state.[28] Figure 6 shows the variation of the wave function under the e_2' distortion. It should be noted that in both the radical and cation the stabilizing mode of distortion is the same, although the effect on the energy is first order in the radical and second order in the cation.

Von Neumann–Wigner Distortions. Herzberg and Longuet-Higgins discussed the example of the HNO molecule.[4] For the linear molecule the lowest energy at large HN distances corresponds to the repulsive $^2\Pi$ state. At smaller distances the attractive interaction with the hydrogen causes the $n\pi^*$ excited $^2\Delta$ state to be stabilized and lie lower. When plotted against the NH distance this crossing between states of different symmetry is allowed, but when bending is considered the Π and Δ states both split into A′ and A″ states. The A′–A′ interaction leads to a double cone structure and a bent $^1A'$ ground-state equilibrium geometry. The A″–A″ interaction leads to a second double cone with the same locus for the apex and a low-energy bent $^1A''$ excited state. This discussion is likely to be oversimplified because of neglect of other states such as $^2\Sigma^-$ which also arise from the $n\pi^*$ excitation of NO and which may lie below $^2\Delta$ at all NH distances.

Tanaka and Davidson[30] described a similar situation for HCO. The linear molecule for large CH distances is of $^2\Sigma^+$ symmetry and is strongly repulsive. The $n\pi^*$ $^3\Pi$ state of CO interacts favorably with hydrogen to give a bonding $^2\Pi$ potential curve. At intermediate values of the CH distance these curves cross, and bending causes the A′ component of the Π state to interact with the $^2\Sigma^+$ state to produce a double cone potential surface and a bent equilibrium geometry. The A″ component of Π has a minimum for the linear molecule.

Several examples of a similar type are known for bent C_{2v} triatomic molecules. Here bending preserves symmetry and often leads to crossing of surfaces of different C_{2v} symmetry. Upon asymmetric stretch the A_2 and B_1 states mix, as do the A_1 and B_2 states. This often gives rise to a double cone potential surface and complex vibration spectra. The best known example[31] of this type is NO_2. For this molecule the weakly antibonding a_1 orbital that is largely localized on nitrogen, the $n_-(b_2)$ combination of oxygen nonbonding n orbitals, and the $\pi_-(a_2)$ nonbonding combination of oxygen π orbitals are very similar in energy. At large bond angles the b_1 antibonding π orbital is also low in energy. In the lowest states of NO_2, five electrons are in these orbitals. At large bond angles (>112°) the lowest state is $b_2^2a_2^2a_1^1$ $^2A_1$ and the second state is $b_2^2a_2^2b_1^1$ $^2B_1$. At small bond angles the oxygen nonbonded orbitals are destablized while the a_1 orbital is stabilized so the lowest state is $b_2^1a_2^2a_1^2$ $^2B_2$ and the second state is $b_2^2a_2^1a_1^2$ $^2A_2$. Thus, two crossings occur with O–N–O bond angle changes. Hence, asymmetric stretch leads to double cone structures mixing $^2A_1$ with $^2B_2$ and $^2B_1$ with $^2A_2$. On the lower $^2A_1$–$^2B_2$ surface the lowest $^2B_2$ C_{2v} point is a saddle point and there is an all downhill path from this point to the $^2A_1$ minimum via the "pseudo-rotation" motion along a trough which passes through geometries with unequal bond lengths. This surface is shown schematically in Figure 7.

This behavior of NO_2 is also seen in some of the excited states of O_3 and SO_2, as well as the ground state of the HCO_2 radical. In all of these molecules the a_1, b_2, and a_2 orbitals are nearly degenerate. For HCO_2 the a_1 orbital is stabilized by the bond to the hydrogen compared to NO_2 so the $a_1^2b_2^1$ $^2B_2$ state is lowered compared to $a_1^1b_2^2$ $^2A_1$. The best calculations[32] for HCO_2 show the same double cone structure as NO_2 but the $^2B_2$ C_{2v} structure is now the lowest point in the trough and $^2A_1$ is the saddle point. The pseudo-rotation valley is extremely flat, however, compared to NO_2. HCO_2 also has a low-energy $^2A_2$ state but $^2B_1$ is fairly high in energy. For O_3 or SO_2 one would expect low-energy excitation from a_1, b_2, or a_2 into the b_1 π^* orbital. As for NO_2 the a_1^1 $^{1,3}B_1$ and b_2^1 $^{1,3}A_2$ states will intersect as a function of bond angle and will interact strongly upon bending. The a_2^1 $^{1,3}B_2$ states are only a little higher in energy. The observed asymmetric stretch vibrational structure is irregular[33] for the SO_2 $^3B_1$ state. Because of the large $\pi\pi^*$ exchange integral $^3B_2$ is nearly as low as $^3B_1$ or $^3A_2$ while $^1B_2$ is fairly high in energy.[34]

In a more complicated example we located a crossing between ^1A_g and $^1B_{2u}$ at some D_{2h} geometries of 1,3-dimethylenecyclobutadiene.[35] The bonding in these states is shown schematically in Figure 8. At the crossing points the degeneracy could be lifted by a b_{2u} distortion that reduced the molecular symmetry to C_{2v} and allowed the two states (both $^1A_1$ in C_{2v}) to mix. The energy lowering was linear in the distortion coordinate, as expected for a first-order Jahn–Teller effect.

At D_{2h} geometries removed somewhat from the crossing

(27) Borden, W. T.; Davidson, E. R. *J. Am. Chem. Soc.* **1980**, *102*, 7958.
(28) Borden, W. T.; Davidson, E. R. *J. Am. Chem. Soc.* **1979**, *101*, 3771.
(29) Liebling, G. R.; McConnell, H. M. *J. Chem. Phys.* **1965**, *42*, 3931.
(30) Tanaka, K.; Davidson, E. R. *J. Chem. Phys.* **1979**, *70*, 2904.
(31) Jackels, C. F.; Davidson, E. R. *J. Chem. Phys.* **1976**, *64*, 2908. **1976**, *65*, 2941.
(32) Feller, D.; Huyser, E. S.; Borden, W. T.; Davidson, E. R. *J. Am. Chem. Soc.* **1983**, *105*, 1459.
(33) Mulliken, R. S. *Can. J. Chem.* **1958**, *36*, 10.
(34) Phillips, P.; Davidson, E. R. *J. Comput. Chem.* **1983**, *4*, 337.
(35) Davidson, E. R.; Borden, W. T.; Smith, J. *J. Am. Chem. Soc.* **1978**, *100*, 3299.

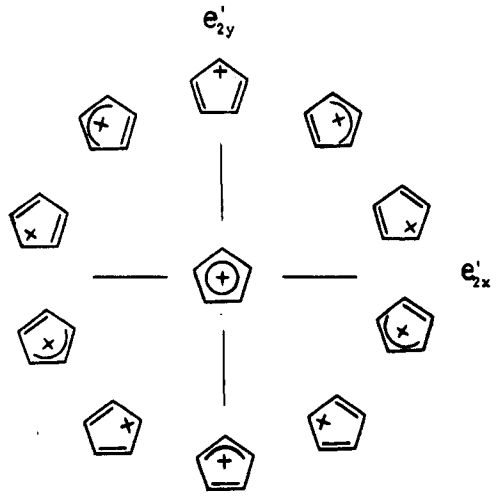

Figure 6. The variation of the bonding in the $^1E_2'$ wave function of cyclopentadienyl cation as a function of e_2' stretching of the CC bonds.

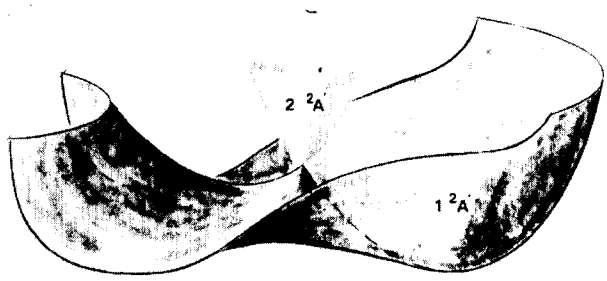

Figure 7. A schematic representation of the $^2A'$ ground-state potential surface of NO_2. The minimum corresponds to $^2A_1$ and the saddle point to $^2B_2$.

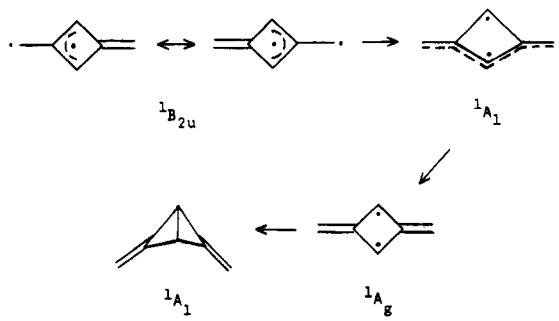

Figure 8. A schematic representation of the bonding in the wave functions at some points on the ground-state potential surface of 1,3-dimethylenecyclobutadiene.

points, b_{2u} distortion still produced an energy lowering, but one that was quadratic in the distortion coordinate as expected from eq 2. It was shown that the lowest singlet surface for 1,3-dimethylenecyclobutadiene could be nicely fit by a two-state model. The crucial parameter for determining the favorability of a b_{2u} distortion from D_{2h} symmetry was the energy separation between ^1A_g and $^1B_{2u}$, which was a function of the distance along an a_{1g} coordinate from the point of intersection.

The true ground state for the planar molecule is actually the triplet state. When nonplanar distortions are allowed for the singlet state, the molecule tends to fold and form a long cross-ring bond. This folded singlet state is close to the triplet state in energy.[36]

(36) Feller, D.; Davidson, E. R.; Borden, W. T. *J. Am. Chem. Soc.* **1982**, *104*, 1216.

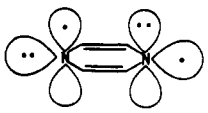

Figure 9. The broken symmetry wave function for the $^3n\pi^*$ state of pyrazine.

Instability Problems

Nearly all of the examples discussed above exhibit artifactual structure for the Hartree–Fock wave function. In some cases this artifactual character persists for MCSCF or limited CI calculations.

Allyl is well-known to exhibit a "doublet instability" at the restricted Hartree–Fock level of theory.[37] That is, at C_{2v} geometries the RHF wave function will break symmetry unless constrained, and the RHF potential surface has a cusp at C_{2v} with a pair of equivalent asymmetric minima corresponding to the valence bond resonance structures C=C–C· and ·C–C=C. Either UHF, MCSCF, or CI in the conceptual minimum basis set π space yields a single minimum.

The isoelectronic CH_2CHO radical exhibits a doublet instability for the $^2A''$ state even though it has no left–right symmetry.[38] The best calculation for the $^2A''$ state shows it to have the unpaired π electron largely localized on carbon. This π state lies below the lowest $^2A'$ σ state.

As discussed above,[32] the isoelectronic HCO_2 radical also has a low-energy $^2A''$ π state. This exhibits a more pronounced doublet instability than allyl due to a decreased resonance energy. However, the largest doublet instability in the HCO_2 radical is found for the $^2A'$ ground state. Only very high level wave functions that include σ–π correlation predict the σ ground state to have C_{2v} symmetry.

In the isoelectronic NO_2 radical the RHF solution is stable at large bond angles for the $^2A_1$ ground state. At small bond angles, where $^2B_2$ is the lowest state, there is a pronounced doublet instability. When the doublet instability problem is overcome by MCSCF or CI, so that the energy gradient vanishes at the $^2B_2$ C_{2v} geometry, this geometry is still found to be a saddle point in NO_2. The possibility of an allyl-like doublet instability in the $^2B_1$ state of NO_2 does not seem to have been examined. This type of instability also persists in the $^3n_{\pm}\pi^*$ excited states of SO_2 and makes it difficult to predict whether or not these excited states have C_{2v} symmetry.[34]

Excitations out of equivalent weakly interacting lone pairs are, as discussed for NO_2, SO_2 and HCO_2, particularly prone to symmetry breaking. When the lone pairs are even more isolated from each other as in pyrazine the effect is amplified with $^3n_{\pm}\pi^*$ calculations yielding the localized structure[39] shown in Figure 9.

Even fairly large MCSCF calculations persist in giving broken symmetry wave functions at D_{2h} geometries so that theoretical determination of the equilibrium geometry is difficult. If the lone pairs are sufficiently noninteracting it is certain that the molecule will actually break symmetry.[40] Nevertheless, at symmetrical geometries the exact wave functions must transform like irreducible representations of the point group. When they do not, the geometry predictions are suspect.

Artifactual symmetry breaking is also prevalent in E states of molecules.[14] If the symmetry unconstrained wave

(37) Paldus, J.; Veillard, A. *Mol. Phys.* **1978**, *35*, 445.
(38) Huyser, E. S.; Feller, D.; Borden, W. T.; Davidson, E. R. *J. Am. Chem. Soc.* **1982**, *104*, 2956.
(39) Ellenbogen, J. C.; Feller, D.; Davidson, E. R. *J. Phys. Chem.* **1982**, *86*, 1583.
(40) Nitzsche, L. E.; Davidson, E. R. *Chem. Phys. Lett.* **1978**, *58*, 171. They discuss a similar result for $^3\pi\pi^*$ states of glyoxal.

functions are not degenerate at a geometry where they should be of E symmetry, then the valley in the resulting Jahn–Teller surface may be distorted toward the wrong geometry or may overestimate the barrier to pseudo-rotation. Examples of this phenomenon, discussed above, include trimethylenemethane, cyclopropenyl anion [and the isoelectronic $(NH)_3^{2+}$], and cyclobutadiene radical cation.

ARTICLES

Fluorescence of Polymerized Diacetylene Bilayer Films

John Olmsted III* and Margith Strand

Chemistry Department, California State University, Fullerton, California 92634 *(Received: November 15, 1982; In Final Form: March 10, 1983)*

Monolayer films of 27-carbon-chain-length alkyldiacetylenecarboxylic acid, $C_{14}H_{29}C{\equiv}C{-}C{\equiv}CC_8H_{16}COOH$, can be polymerized on the aqueous surface by UV irradiation. The resulting blue polydiacetylene is readily transferred onto glass slides to form multilayers. The blue form, which absorbs at 640 and 580 nm, is nonfluorescent, but treatment with heat or polar, nonaqueous solvent (e.g., pyridine) irreversibly transforms the polymer to a red form absorbing at 540 and 500 nm. This red form fluoresces with emission maxima at 570 and 640 nm. The fluorescence quantum yield, using cresyl violet and Rhodamine 6G embedded in nail polish films as standards, is measured to be $(2.0 \pm 0.5) \times 10^{-2}$.

Introduction

Films formed from surface-active diacetylene compounds containing long, straight-chain alkyl groups and a polar head group have been shown by several groups to be polymerizable when exposed to UV radiation in the absence of oxygen.[1-3] The resulting polymers display interesting spectral features, being blue upon initial formation and transforming subsequently to a stable red form.[4-6] Fluorescence of polydiacetylenes was first reported qualitatively by Baughman and Chance[7] and has since been reported for water-soluble urethane-substituted systems,[8] a polymer containing chiral centers,[9] and an amphiphilic system.[10] For all cases studied thus far, the longer wavelength absorbing form of the polymer formed initially upon irradiation shows negligible fluorescence, significant emission occurring only after the polymer is converted to a form showing blue-shifted absorption. In none of the work reported to date were quantitative fluorescence data presented. Because bilayers formed from such polymerized diacetylene films display remarkable strength allowing them to span macroscopic holes,[3] we have undertaken studies to determine their suitability as support structures for immobilized photosensitizers. As part of those studies, we have examined the luminescence of the polymer chromophore, which is the subject of this communication.

Procedures and Results

The diacetylene monomer of formula $H_3C(CH_2)_{13}{-}C{\equiv}C{-}C{\equiv}C{-}(CH_2)_8COOH$ was prepared from 10-undecynoic acid and 1-hexadecyne (both from Farchan Labs, Willoughby, OH). Hexadecyne was treated with mercuric acetate to yield the mercuric diacetylide, which was then treated with bromine in carbon tetrachloride to give 1-bromohexadecyne.[11] This was chromatographed on Pd–C and then reacted with the undecynoic acid in the presence of Cu^+ to give the diacetylene via Chodkiewicz coupling.[12,13] The resulting crystalline product, after recrystallization from boiling light petroleum ether (30–60 °C), turned the characteristic deep blue color of polymerized diacetylenes upon irradiation with UV light.

Oriented monolayer films of diacetylene monomer were produced by layering a drop of 1 mg/mL solution of the monomer in chloroform on the surface of doubly distilled water, allowing it to spread and the chloroform to evaporate, and then slowly compressing the resulting film until stress patterns began to appear on the surface. Compression was accomplished by drawing ferric stearate

(1) Tieke, B.; Graf, H.-J.; Wegner, G.; Naegele, B.; Ringsdorf, H.; Banerjie, A.; Day, D.; Lando, J. B. *Colloid Polym. Sci.* **1977**, *255*, 521.
(2) Day, D.; Ringsdorf, H. *J. Polym. Sci., Polym. Lett. Ed.* **1978**, *16*, 205.
(3) Day, D.; Lando, J. B. *Macromolecules* **1980**, *13*, 1478.
(4) Day, D.; Ringsdorf, H. *Makromol. Chem.* **1979**, *180*, 1059.
(5) Day, D.; Hub, H. H.; Ringsdorf, H. *Isr. J. Chem.* **1979**, *18*, 325.
(6) Tieke, B.; Lieser, G.; Wegner, G. *J. Polym. Sci., Polym. Chem. Ed.* **1979**, *17*, 1631.
(7) Baughman, R. H.; Chance, R. R. *J. Polym. Sci., Polym. Phys. Ed.* **1976**, *14*, 2037.
(8) Bhattacharjee, H. R.; Preziosi, A. F.; Patel, G. N. *J. Chem. Phys.* **1980**, *73*, 1478.
(9) Wilson, R. B.; Duesler, E. N.; Curtin, D. Y.; Paul, I. C.; Baughman, R. H.; Preziosi, A. F. *J. Am. Chem. Soc.* **1982**, *104*, 509.
(10) Bubeck, C.; Tieke, B.; Wegner, G. *Ber. Bunsenges. Phys. Chem.* **1982**, *86*, 495.
(11) Eglington, G.; McCrae, W. *J. Chem. Soc.* **1963**, 2295.
(12) Chodkiewicz, W. *Ann. Chim. (Paris)* **1957**, *2*, 852.
(13) Eglington, G.; McCrae, W. *Adv. Org. Chem.* **1963**, *4*, 228.

0022-3654/83/2087-4790$01.50/0